Journal of Engineering and Technology for Industrial Applications

ITEGAM-JETIA

Manaus, v10. n.50, p. 168-174. November/ December., 2024.
DOI: https://doi.org/10.5935/jetia.v10i50.1271

ISSN ONLINE: 2447-0228

RESEARCH ARTICLE OPEN ACCESS

ENHANCED ESTIMATION OF TORQUE BASED ON COGNITIVE TRAINING MODEL FOR ROBUST PMSM IN EV APPLICATIONS

G. Sudeep[1], J. N. and Chandra Sekhar[2]

[1,2] Department of EEE, Sri Venkateswara University, Tirupati, India

[1] http://orcid.org/0009-0005-0619-7996 , [2]http://orcid.org/0000-0003-2767-2467

Email: gaduputisudeep@gmail.com, chandu.jinka@gmail.com

ARTICLE INFO

Article History
Received: August 29, 2024
Revised: October 1, 2024
Accepted: November 10, 2024
Published: December 31, 2024

Feedforward Neural Network (FNN),
Permanent Magnet Synchronous Motors (PMSM),
Hyperband Algorithm.

ABSTRACT

Permanent Magnet Synchronous Motors (PMSM) which are used in commercial applications, requires precise torque calculation, which is necessary for the intended control. Conventional Model Predictive Control (MPC) performance is hampered by model parameter mismatches and high computational demands, precise torque control often necessitates the knowledge of rotor speed and position, which are traditionally obtained using mechanical sensors. The paper proposes Feedforward Neural Network model to estimate the parameter for desired switching of inverter for accurate position of rotor in optimized time. However, this model uses the d-q axis currents, voltages, rotor angle as inputs, and electromagnetic torque as the output. The model is developed with the help of Python programming based on Hyperband algorithm for hyperparameter tuning. Hyperband algorithm, efficiently optimizes hyperparameters by adaptive resource allocation, early stopping, reducing training time and improving accuracy. This integration allows the neural network(NN) to dynamically optimize its architecture, ensuring precise torque estimation. This approach addresses computational challenges and enhances the system's efficiency and responsiveness to real-time parameter variations and disturbances, leading to more robust and high-performing motor control applications.

I. INTRODUCTION

Electric vehicles (EVs) have emerged as a promising solution to address the growing concerns over environmental pollution and energy sustainability. PMSM have become a popular choice for EV propulsion systems [1] due to their high-power density, efficiency, and wide constant power speed range. The PMSM can provide high torque at low speeds, making them suitable for urban driving conditions. In addition, their compact size and lightweight design make them ideal for integration into the limited space available in EV.

One of the key aspects of utilizing PMSM in EV is the precise control of torque. The torque control in PMSM drives is crucial for achieving optimal performance and efficiency in EV propulsion systems. To achieve effective torque control, various control strategies can be employed, such as field-oriented control (FOC) or direct torque control (DTC) [2]. Advancements in motor control algorithms and sensor technologies have enhanced the accuracy and responsiveness of torque control in PMSM drives, leading to improved overall system efficiency and performance [3]. The integration of advanced sensor technologies has significantly enhanced the accuracy and responsiveness of torque control in PMSM drives. This level of control ensures smooth operation and optimal performance, further contributing to the overall efficiency of electric vehicle propulsion systems. In addition to advanced sensor technologies, there have been significant developments in sensor less control techniques for PMSM in EV. These techniques use algorithms and mathematical models to estimate the motor's operating conditions and rotor position without the need for physical sensors, thereby reducing cost and complexity in EV propulsion systems [4]. The offline torque estimation using sensors and torque transducers provides the necessary data for optimizing torque control strategies, ensuring that the PMSM meet the dynamic power requirements of electric vehicle propulsion systems. This approach further contributes to the smooth operation and overall efficiency of EV, addressing the specific needs of urban driving conditions and improving the driving experience for users [5]. Online torque estimations enable real-time monitoring and adjustment of torque in PMSM drives, ensuring optimal power

delivery and responsiveness to dynamic power requirements. By incorporating advanced algorithms and sensor feedback, online torque estimations contribute to the seamless operation of EV in varied driving conditions, including urban settings with frequent starts and stops. One such approach is the use of Kriging-based techniques for online torque calculation in brushless DC motors, as highlighted in [6]. By leveraging improved estimation techniques, EV equipped with PMSMs can achieve enhanced performance and responsiveness, particularly in urban settings with frequent starts and stops.

Deep learning models, such as convolutional NN and recurrent NN, can be utilized to analyze and learn from large datasets of motor parameters and operating conditions. By training these models on a diverse set of torque measurements and corresponding motor states, the deep learning approach can provide accurate and real-time torque estimations for PMSMs in EV [7]. The block diagram Figure 1 depicts a system for controlling a PMSM. It includes components for current and voltage measurement, voltage source inverter, electrical angle measurement, sector identification, and lookup tables for estimators, ensuring accurate motor control and performance optimization.

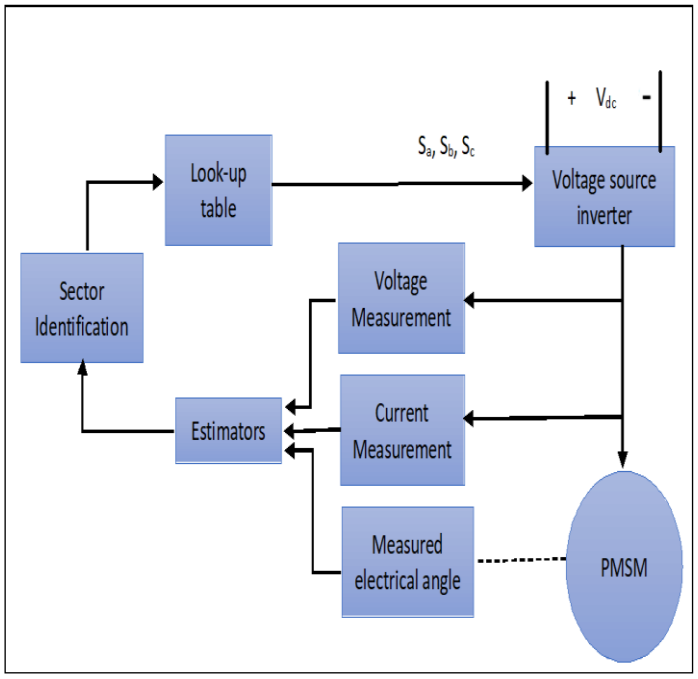

Figure 1: Torque control of PMSM Drive.
Source: Authors, (2024).

Accurately estimating motor torque is essential for the efficient control of PMSM. Torque estimation methods are generally categorized into online and offline techniques. Online methods use real-time electrical parameters—such as voltages, currents, and rotor position—to calculate instantaneous torque, offering the benefit of reduced system complexity and cost by eliminating the need for additional sensors. Offline methods, however, rely on detailed motor characterization through complex models and extensive testing. Although more complex, offline techniques can yield higher accuracy, particularly for motors with intricate magnetic structures. The choice between these methods depends on the application's specific needs, balancing complexity, cost, and accuracy.

Table 1: Related Literature Review.

Reference	Strength of Review
[8]	Suggests a technique for improving the identification of PMSM motor parameters through the use of a Chaotic Artificial Fish Swarm Algorithm (CAFSA) to optimize initial weights in a Back Propagation Neural Network (BPNN).
[9]	Introduces a sensor less speed tracking control method using polynomial equations and sliding mode-based control, validated on an embedded board.
[10]	Develops a feedforward NN for PMSM temperature estimation, achieving closed-loop errors under 4.5°C.
[11]	Assesses deep recurrent and convolutional NN with residual connections for PMSM temperature prediction, offering high performance without domain expertise.
[12]	Introduces sensor less robust optimum control strategy for PMSM with NN-based observers, validated by comparison tests and simulations.

Source: Authors, (2024).

The structure of this document is as follows. The suggested methodology framework is explained in Section 2, the results and discussion are covered in Section 3, and the conclusion is provided in Section 4.

II. PROPOSED METHODOLOGY

II.1 FRAME WORK FOR PROPOSED METHODOLOGY

This study presents a machine learning (ML) method for precise PMSM torque prediction. Data on currents, voltage and torque are collected cleaned and standardized. The model undergoes hyperparameter tunning and iterative training, with performance evaluated using R^2. Figure 2 visualization support model analysis, aiming to enhance motor control and optimization.

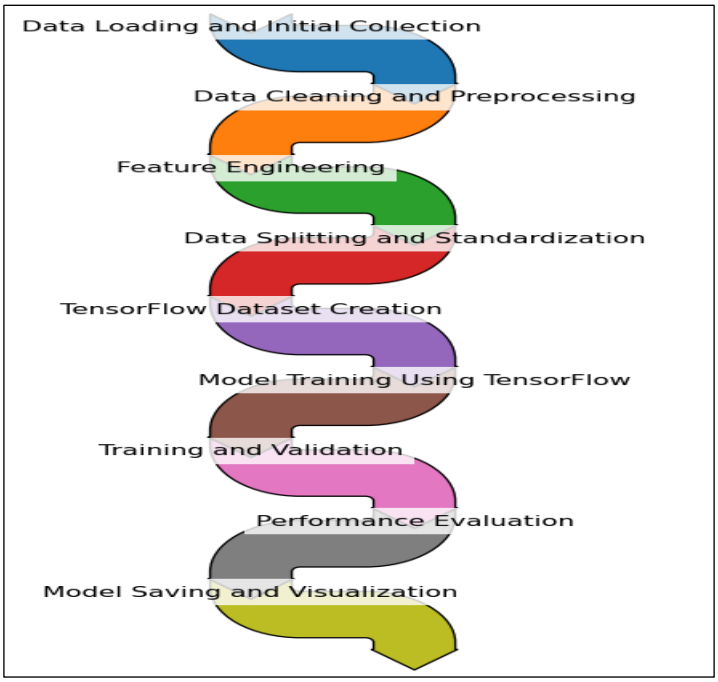

Figure 2: Flow chart of Proposed Methodology.
Source: Authors, (2024).

II.2. TORQUE ESTIMATION IN PMSM

Performance and efficiency can be significantly increased by integrating torque estimation techniques with PMSM control. For example, the application of DTC strategies—which can offer better dynamic responsiveness and fault tolerance than conventional vector control methods—can be made possible by the availability of correct torque information. Furthermore, the use of torque estimation in engine speed control can contribute to enhanced engine performance and efficiency, as demonstrated in the application of nonlinear observer-based torque estimation for engine speed control.

One widely adopted approach is to utilize the Clark and Park transformations to simplify the PMSM model and enable the implementation of field-oriented control techniques. The Clark transformation converts the three-phase stator voltages and currents into their equivalent two-phase stationary reference frame components, while the Park transformation further transforms these components into a synchronously rotating reference frame, relationships is explained in figure 3.

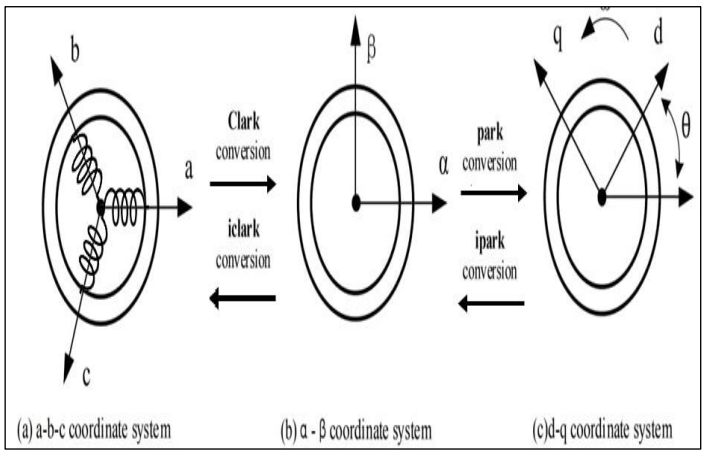

Figure 3: Transformation relationship in PMSM.
Source: Authors, (2024).

$$\begin{bmatrix} u_a \\ u_b \\ u_c \end{bmatrix} = \begin{bmatrix} R & 0 & 0 \\ 0 & R & 0 \\ 0 & 0 & R \end{bmatrix} \begin{bmatrix} i_a \\ i_b \\ i_c \end{bmatrix} + \begin{bmatrix} L & 0 & 0 \\ 0 & L & 0 \\ 0 & 0 & L \end{bmatrix} \frac{d}{dt} \begin{bmatrix} i_a \\ i_b \\ i_c \end{bmatrix} + \Phi\omega \begin{bmatrix} \sin \omega t \\ \sin(\omega t - 2\pi/3) \\ \sin(\omega t + 2\pi/3) \end{bmatrix} \quad (1)$$

$$\begin{bmatrix} i_\alpha \\ i_\beta \end{bmatrix} = \sqrt{\frac{2}{3}} \begin{bmatrix} 1 & -\frac{1}{2} & -\frac{1}{2} \\ 0 & \frac{\sqrt{3}}{2} & -\frac{\sqrt{3}}{2} \end{bmatrix} \begin{bmatrix} i_a \\ i_b \\ i_c \end{bmatrix} \quad (2)$$

$$\begin{bmatrix} i_a \\ i_b \\ i_c \end{bmatrix} = \sqrt{\frac{2}{3}} \begin{bmatrix} 1 & 0 \\ -\frac{1}{2} & \frac{\sqrt{3}}{2} \\ -\frac{1}{2} & -\frac{\sqrt{3}}{2} \end{bmatrix} \begin{bmatrix} i_\alpha \\ i_\beta \end{bmatrix} \quad (3)$$

$$\begin{bmatrix} i_d \\ i_q \end{bmatrix} = \begin{bmatrix} \cos\theta & \sin\theta \\ -\sin\theta & \cos\theta \end{bmatrix} \begin{bmatrix} i_\alpha \\ i_\beta \end{bmatrix} \quad (4)$$

$$\begin{bmatrix} i_\alpha \\ i_\beta \end{bmatrix} = \begin{bmatrix} \cos\theta & -\sin\theta \\ \sin\theta & \cos\theta \end{bmatrix} \begin{bmatrix} i_d \\ i_q \end{bmatrix} \quad (5)$$

In a PMSM, L represents the magnetic flux generated by the stator's permanent magnet and u_a, u_b and u_c are the voltages in each phase of the stator winding within a three-phase coordinate system. Similarly, i_a, i_b and i_c indicate the phase currents in this system, while R refers to the resistance of each stator winding phase. The three-phase voltage equations of a PMSM are inherently differential equations, which makes direct solutions complex and challenging. The angular velocity of rotation within the a-b-c coordinate system is denoted by ω. To effectively simplify the problem and enhance the motor's control capabilities, a suitable transformation is required to decouple these variables. This transformation process for the PMSM, which involves converting between various coordinate systems, is guided by the principles of preserving equivalent current, voltage, flux, and magnetomotive force. For instance, the Park transform converts the voltage model from the rotating d-q coordinate system to a form easier to manage, while the Clark transform shifts from the space vector to the a-b-c coordinate system for the static two-phase voltage model (α, β). These transformations yield a voltage model similar to that of a two-phase DC motor, making it easier to control. The transformations help determine the phase angle θ between the d-axis and q-axis, which is crucial for accurate motor control. Equations (2) through (5), in that order, display the park transformation relations between current and the Clark transformation in each coordinate system. Similar results can be obtained for the voltage transformation relationship in each coordinate system.

II.3. IMPLEMENTATION OF POLYNOMIAL LINEAR REGRESSION MODEL

The desired response for the variable PLRM is obtained using the estimated torque control, while the regressors are the observed torque and speed. The mathematical expectation of items with a higher order, k =0 in Equation (6), which presents the torque curve with respect to observed torque and speed, may then be fitted. It is assumed that the population size for things with a higher order "k" is minimal. But, bivariate k[th]-order PLRM [13], is the equation (6) is known as.

$$T_{cij} = \sum_{\gamma=0}^{k} \sum_{\lambda=0}^{k} \beta_{\gamma\lambda} T_{mij} \lambda + \varepsilon_{ij} \quad (6)$$

Where must be k≥1, and i = 1,2,……n & j = 1,2,…..q

When $\beta_{\gamma\lambda}$ is the regression coefficient that needs to be determined, ε_{ij} is the torque error, and each εij is independent and has the same distribution. to acquire the linear regression of second order polynomials. In equation (6), the value of k is 2. Equation 2 shows how to use the regressors of the observed torque and speed to create the bivariate second order PLRM.

$$T_{cij} = \beta_{00} + \beta_{01}\omega_i + \beta_{02}\omega_i^2 + \beta_{10}T_{mij} + \beta_{11}T_{mij}\omega_i + \beta_{20}T_{mij}^2 + \varepsilon_{ij} \quad (7)$$

$$\text{where} T_{mij} = \begin{bmatrix} x_{i100} & x_{i101} & x_{i102} & x_{i110} & x_{i11} & x_{i120} \\ x_{i200} & x_{i201} & x_{i202} & x_{i210} & x_{i211} & x_{i220} \\ \vdots & \vdots & \vdots & \vdots & \vdots & \vdots \\ x_{iq00} & x_{iq01} & x_{iq02} & x_{iq10} & x_{iq11} & x_{iq20} \end{bmatrix} \quad (8)$$

$$\beta = [\beta_{00} \quad \beta_{01} \quad \beta_{02} \quad \beta_{10} \quad \beta_{11} \quad \beta_{20}]^T \quad (9)$$

The value of ω_i in equation (8) is 0. After that, as equation (10) shows how to generate the univariate second order PLRM using the observed torque's regressor. One way to rewrite equation (9) is as equation (11) shows.

$$T_{cij} = \beta_{00} + \beta_{10}T_{mij} + \beta_{20}T_{mij}^2 + \varepsilon_{ij} \quad (10)$$

$$\beta = [\beta_{00} \quad \beta_{10} \quad \beta_{20}]^T \quad (11)$$

II.4. IMPLEMENTATION OF DEEP LEARNING TECHNIQUE

The integration of deep learning with motor control systems holds the potential to revolutionize the field of PMSM torque estimation. It not only contributes to enhanced performance and energy efficiency but also facilitates the development of intelligent and autonomous electromechanical systems [14]. In this study, we explore the implementation of ML algorithms for torque estimation in PMSMs. Deep Learning models, especially NN, have emerged as an effective tool for accurate torque estimation in PMSMs.

Since the selection of hyperparameters can have a substantial impact on the model's performance, hyperparameter tuning in NN is an essential step in the creation of ML models. In particular for complicated models with several hyperparameters, traditional hyperparameter optimization techniques like grid search and random search can be computationally costly and time-consuming. [15]. To address this challenge, the Hyperband algorithm has been proposed as a novel and efficient approach to hyperparameter optimization shown in Figure 4 NN structure.

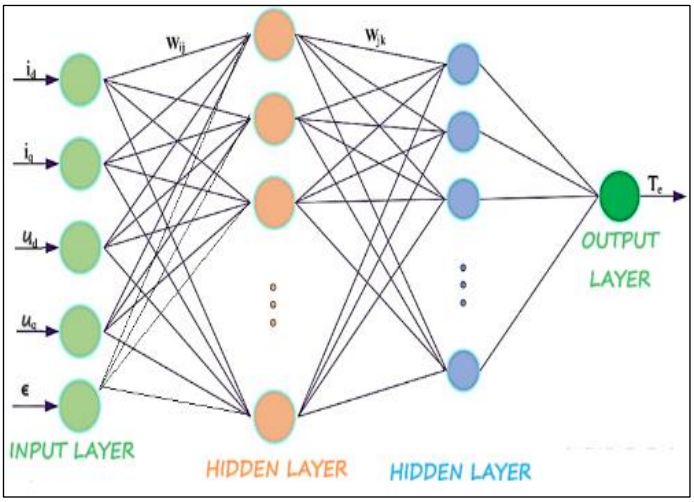

Figure 4: Neural Network Structure.
Source: Authors, (2024).

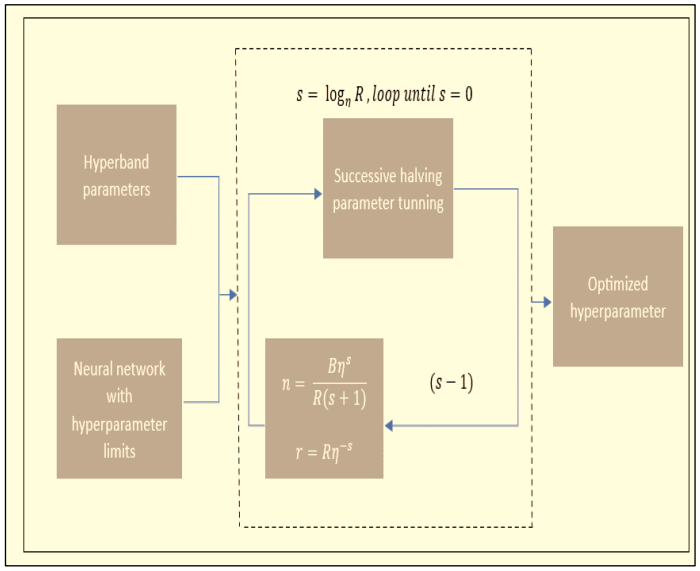

Figure 5: Hyperparameter optimization.
Source: Authors, (2024).

Scholars have investigated diverse methodologies for optimizing hyperparameters, encompassing extensive trials to comprehend the impacts of distinct hyperparameters and their mutual relations. Figure 5 illustrates one such strategy called Hyperband, a cutting-edge bandit-based technology that can offer appreciable speedups over conventional optimization techniques.

III.1 RESULTS AND DISCUSSION

III.1. DATA SET

This article proposes a comprehensive analysis on two datasets, namely Dataset 1 and Dataset 2, which contain measurements such as, the target variable torque T in Nm [16][17]. The dataset statistics as shown in figure 6 supports the torque T in Nm are as follows:

- Dataset 1: The dataset consists of 37 million samples with a mean value of -0.86 Nm and a standard deviation of 71.39 Nm. The minimum and maximum values are -133.90 Nm and 134.07 Nm, respectively. The interquartile range (IQR), spanning from the 25th percentile (-56.13 Nm) to the 75th percentile (55.40 Nm), indicates a wide spread of data points around the median (-1.08 Nm).
- Dataset 2: Similar to Dataset 1, this dataset also contains 37 million samples. The mean value is slightly lower at -0.90 Nm, with a higher standard deviation of 72.51 Nm. The minimum and maximum values are -136.84 Nm and 136.04 Nm, respectively. The IQR for Dataset 2 is slightly broader, with the 25th percentile at -59.40 Nm and the 75th percentile at 57.54 Nm, and a median of -1.37 Nm.

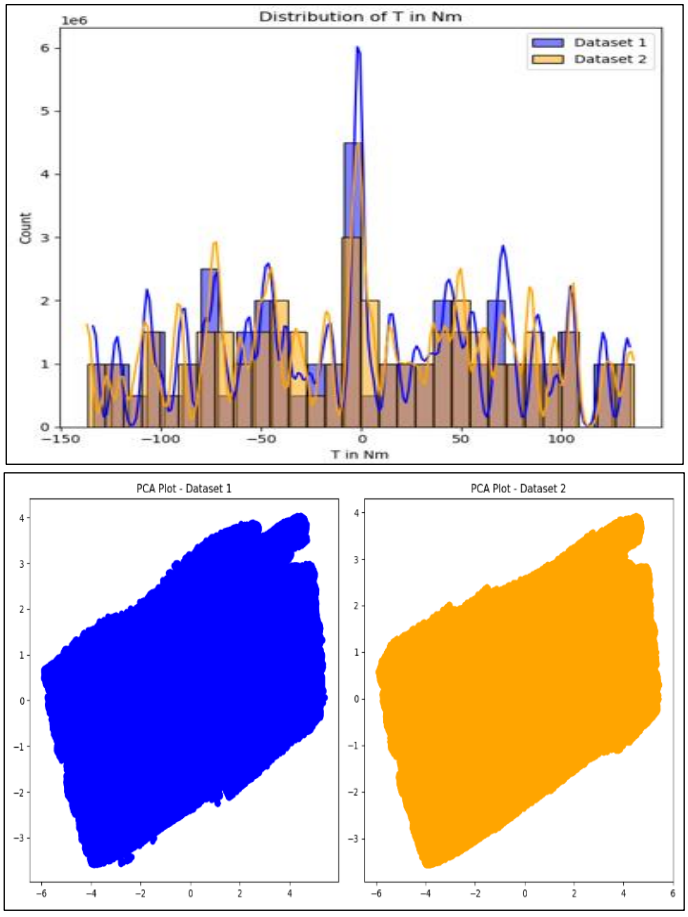

Figure 6: Dataset visualization.
Source: Authors, (2024).

III.2. RESULTS

The training process of the NN model loss values for both the training and validation datasets over 15 epochs. The tuning process yielded the following optimal hyperparameters:

Number of Neurons: 42, Layers: 8 and Learning Rate: 0.001, The model's training and validation loss over a period of 15 epochs conducted on dataset (2000RPM) is displayed in Figure 7 was developed in python version 3.12 with the help of keras tuner tool. Within the first few epochs, the model shows a quick decrease in both training and validation loss, followed by a stable plateau, suggesting that the model converged successfully and that there was not a large amount of overfitting during training Each hidden layer's dense component has 1,806 parameters (42 inputs * 42 outputs + 42 biases), while the output layer has 43 parameters (42 inputs * 1 output + 1 bias), leading to a total of 14,785 trainable parameters in the network. The developed model was pre-trained on NN was employed and subsequently trained on to adapt to a similar distinct dataset (120RPM). This process was carried out using TensorFlow with a distributed training strategy to optimize the model's performance. The training and validation loss over a period of 15 epochs is depicted in the graph as shown in figure 8. Early on, both losses exhibit a notable decline, pointing to a quick convergence of the model. The model may be well-tuned and not overfit if the validation loss is continuously less than the training loss. This steady performance demonstrates the resilience and generalizability of the approach.

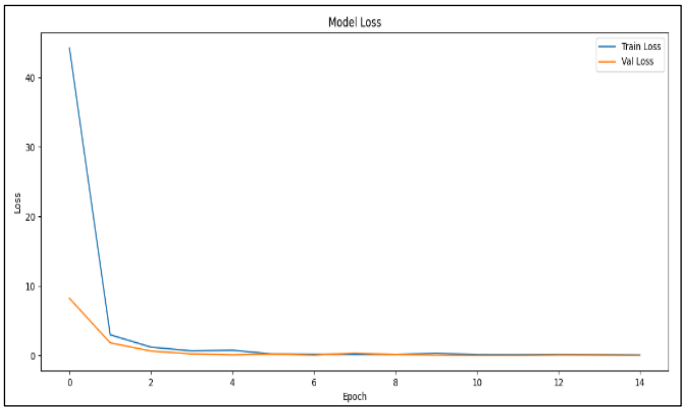

Figure 7: Loss curves for 2000RPM.
Source: Authors, (2024).

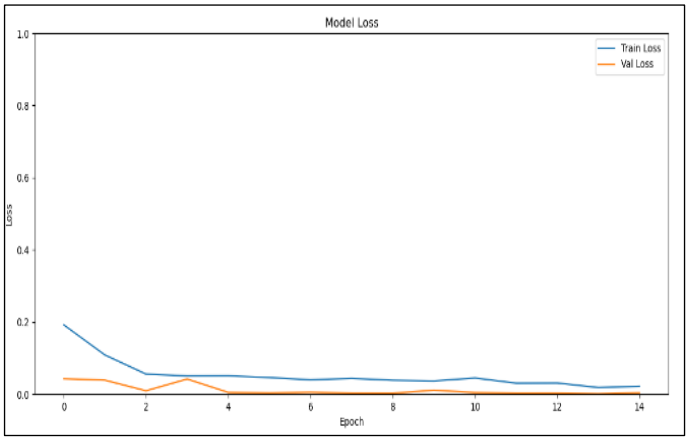

Figure 8: Loss curve for 120RPM.
Source: Authors, (2024).

Tables 2 and 3 compare the performance of polynomial linear regression and a fully connected feedforward neural network (NN) for torque estimation at two different speeds: 120 RPM and 2000 RPM. Table 2 shows that polynomial linear regression yields relatively high Mean Squared Error (MSE), Root Mean Squared Error (RMSE), and Mean Absolute Error (MAE) values, with MSEs of 212.850 and 206.064 at 120 RPM and 2000 RPM, respectively. These values indicate a moderate level of prediction accuracy, further corroborated by the R-squared values of 0.958 and 0.9608, suggesting that the model explains a substantial portion of the variance in the data but leaves some room for improvement. In contrast, Table 3 presents the results for the fully connected feedforward NN, which demonstrates significantly lower error metrics at both speeds. The MSE is reduced to 0.0009 at 120 RPM and 0.0093 at 2000 RPM, with corresponding RMSEs of 0.0301 and 0.0963. The MAE values are also much lower, at 0.0192 and 0.0542, respectively. The near-perfect R-squared values of 0.999 at both speeds indicate that the NN model almost entirely captures the variance in the dataset, showcasing its superior predictive capabilities over polynomial linear regression for this application. Overall, the NN model provides more accurate and reliable torque estimation across different speeds, making it a more suitable choice for this specific task compared to polynomial linear regression.

Table 2:Polynomial Linear Regression (Tourque Estimation).

Speed	MSE	RMSE	MAE	R-square
RPM 120	212.850	14.589	10.949	0.958
RPM 2000	206.064	14.354	10.714	0.9608

Source: Authors, (2024).

Table 3: Fully connected feedforward NN (Tourque estimation).

Speed	MSE	RMSE	MAE	R-square
RPM 120	0.0009	0.0301	0.0192	0.999
RPM 2000	0.0093	0.0963	0.0542	0.999

Source: Authors, (2024).

The scatter plot presented in Figure 9 and 10 illustrates the relationship between the direct axis current (i_d) and the quadrature axis current (i_q) for the PMSM. The data points, shown as dense clusters, reveal the operational characteristics and current interactions within the motor current dynamics. The plot showcases a distinctive pattern, indicative of the motor's response under varying load conditions and rotational speeds. The clustering and spread of data points highlight the motor's operational envelope and provide insights into the performance and efficiency of the PMSM.

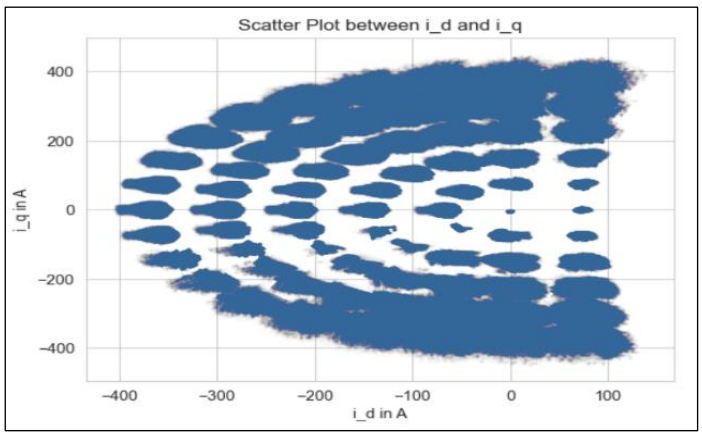

Figure 9: Scatter Plot of i_d vs. i_q for 120RPM.
Source: Authors, (2024).

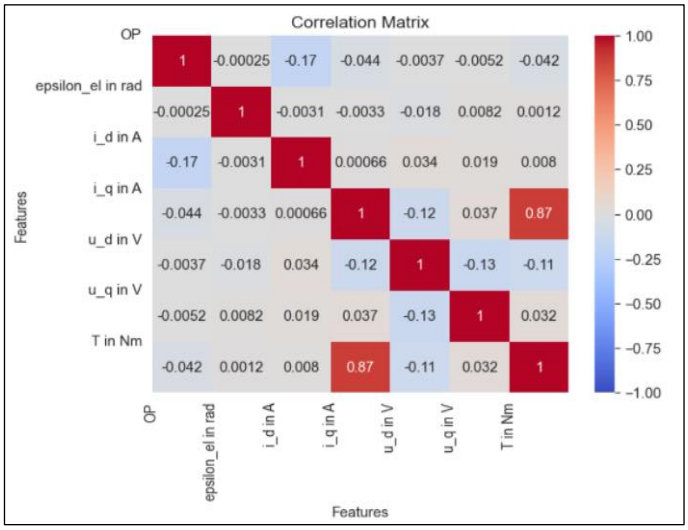

Figure 10: Scatter Plot of i_d vs. i_q for 2000RPM.
Source: Authors, (2024).

Heat Map

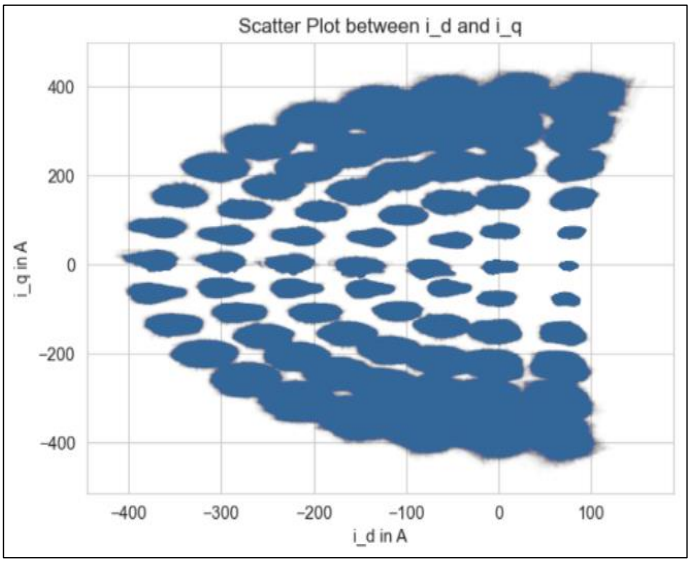

Figure 11: Heat Map at 120RPM.
Source: Authors, (2024).

Case 1: Correlation Matrix Heatmap at 120 RPM

Figure 11 presents the correlation matrix heatmap for various features of the PMSM dataset, including the electrical angle (ϵ_{el}), i_d, i_q, u_d, u_q, and torque (T). This heatmap visually represents the correlation coefficients between these features, providing insights into their linear relationships. The heatmap uses a colour gradient to depict the correlation values, where red shades indicate positive correlations, and blue shades signify negative correlations. The intensity of the colour corresponds to the magnitude of the correlation coefficient, with values ranging from -1 to 1.

Key observations from the heatmap include:

- A strong positive correlation (r=0.87) between the i_q and torque (T), suggesting that as i_q increases, the torque also increases.
- The correlations among other variables, such as i_d, u_d, u_q, and electrical angle(ϵ_{el}), are relatively weak, with coefficients close to zero, signifying little to no linear relationship.

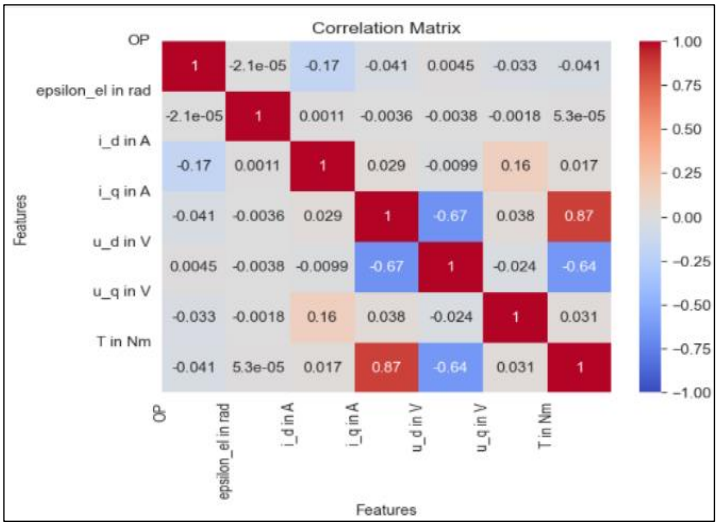

Figure 12: Heat Map at 2000RPM.
Source: Authors, (2024).

Case 2: Correlation Matrix Heatmap at 2000 RPM

Figure 12 shows the correlation matrix heatmap for various features of the PMSM dataset at 2000 RPM, including the electrical angle (ϵ_{el}), i_d, i_q, direct axis voltage (u_d), quadrature axis voltage (u_q), and torque (T).

Key observations from this heatmap include:

- A strong positive correlation (r=0.87) between the i_q and torque (T), indicating that an increase in i_q is associated with an increase in torque.
- A significant negative correlation (r=−0.67) between the u_d and the i_q, suggesting an inverse relationship between these variables.

IV. CONCLUSION

The article demonstrated the effective solution of deep learning for the torque estimation of PMSM. This utilizes the extensive datasets of currents, voltage and rotor angle was implemented in NN model with eight hidden layers, each layer contains 42 neurons. The model demonstrated the superior predictive performance, significantly reducing loss values and attaining high accuracy in torque estimation, outperforming polynomial linear regression models in terms of Mean Squared Error (MSE), Root Mean Squared Error (RMSE), Mean Absolute Error (MAE), and R-square metrics at both 120 RPM and 2000 RPM. Scatter plots of direct axis current (i_d) vs. quadrature axis current (i_q) revealed critical insights into motor behaviour under varying conditions. The investigations underscore the potential of deep learning to improve motor performance, energy efficiency, and operational stability, showcasing NN model in minimizing errors and enhancing torque estimation accuracy. The research enlightened the reputation of advanced ML techniques in industrial automation, offering a promising direction for future research and development in PMSM torque.

V. AUTHOR'S CONTRIBUTION

Conceptualization: G.Sudeep and Dr.J N Chandra sekhar.
Methodology: G.Sudeep and Dr.J N Chandra sekhar.
Investigation: G.Sudeep and Dr.J N Chandra sekhar.
Discussion of results: G.Sudeep and Dr.J N Chandra sekhar.
Writing – Original Draft: G.Sudeep.
Writing – Review and Editing: G.Sudeep.
Resources: Dr.J N Chandra sekhar.

Supervision: Dr.J N Chandra sekhar.
Approval of the final text: G.Sudeep and Dr.J N Chandra sekhar.

VI. ACKNOWLEDGMENTS

The authors would like to express their sincere gratitude to Sri Venkateswara University College of Engineering for providing necessary guidance and support. We are also grateful to the anonymous reviewers for their constructive comments that helped us to improve the quality of this manuscript.

VII. REFERENCES

[1] Z.Q.Zhu, D Howe, "Electrical Machines and drives for Electric, Hybrid and Fuel Cell Vehicles", IEEE vol. 95, no. 95 pp. 746-765 April 2007.

[2] S. D. Pinto, C. Chatzikomis, A. Sorniotti and G. Mantriota, "Comparison of Traction Controllers for Electric Vehicles With On-Board Drivetrains", IEEE Trans., on Vehicular Technology vol. 66, no. 8, pp. 6715-6727, Aug-2017.

[3] M. Dalboni, D.Tavernini, U.Montanaro, A.Soldati, C. Concari, M. Dhaens, A. Sorniotti, "Nonlinear Model Predictive Control for Integrated Energy-Efficient Torque-Vectoring and Anti-Roll Moment Distribution", IEEE Trans., on Mechatronics, vol. 26, no. 3, pp. 1212-1224, June 2021.

[4] T. D. Batzel and K. Lee, "Electric Propulsion With the Sensorless Permanent Magnet Synchronous Motor: Model and Approach", IEEE Trans., on Energy Conversion, vol.20, no.4, pp.818-825, Dec 2005.

[5] S. Shinnaka and S. Takeuchi, "A New Sensorless Drive Control System for Transmissionless EVs Using a Permanent-Magnet Synchronous Motor", World Electr. Veh. J. , 1(1), 1-9, dec 2007**.**

[6] X. Liu, M. Li and M. Xu, "Kriging assisted on-line torque calculation for brushless DC motors used in electric vehicles", IEEE International Symposium on Industrial Electronics, July-2012, 10.1109/ISIE.2012.6237312.

[7] Y. Yan, J. Liang, T. Sun, J. Geng, Gang-Xie, and D. Pan. “Torque estimation and control of PMSM based on deep learning”. Int. Conf. on Electrical Machines and Systems, Dec-2019.

[8] J.W. Jiang, Z. Chen, Y.H. Wang, T. Peng, S.L. Zhu, L.M. Shi “Parameter Estimation for PMSM based on a Back Propagation Neural Network Optimized by Chaotic Artificial Fish Swarm Algorithm” International Journal of Computers Communications & Control, vol.14(6), pp.615-632, December 2019.

[9] Luigi Colombo, Maria Letizia Corradini “An Embedded Strategy for Online Identification of PMSM Parameters and Sensorless Control” IEEE Transactions on control systems technology, vol.27, no.6, pp.2444-2452, Nov-2019.
[10]J Lee, J I Ha, “Temperature Estimation of PMSM Using a Difference-Estimation Feedforward Neural Network” IEEE Access, vol.8, PP.130855-130865, July 2020.

[11] Wilhelm Kirchgässner, Oliver Wallscheid and Joachim Böcker “Estimating Electric Motor Temperatures with Deep Residual Machine Learning” IEEE Trans., on power electronics, vol. 36, no.7, pp.7480-7488, July 2021.

[12] Luy Nguyen Tan, Thanh Pham Cong, Duy Pham Cong “Neural Network Observers and Sensorless Robust Optimal Control for Partially Unknown PMSM with Disturbances and Saturating Voltages” IEEE Trans., on power Electronics, vol. 36, no. 10, pp.12045-12056, Oct-2021.

[13] Hongyu Jie, Gang Zheng “Calibration of Torque Error of Permanent Magnet Synchronous Motor Base on Polynomial Linear Regression Model”, IECON-2019, , October 2019.

[14] L. S. N. D. K. B. S. H. Oscar, "Deep Learning-Based Model Predictive Control for Resonant Power Converters", IEEE Trans., on Industrial Informatics, vol. 17, no.1, pp.409-420, Jan 2021.

[15] T. M. Breuel, "The Effects of Hyperparameters on SGD Training of Neural Networks", arXiv preprint arXiv:1508.02788, 2015, https://doi.org/10.48550/arXiv.1508.02788

[16] A. Brosch, O. Wallscheid, and J. Bocker. Data set: Torque characteristics ¨ of a permanent magnet motor - 74 million samples for data-driven learning. https://tinyurl.com/tt68bpz

[17]A.Brosch, O.Wallscheid and J.Bocker ”Torque and Inductances Estimation for Finite Model Predictive Control of Highly Utilized Permanent Magnet Synchronous Motors”, IEEE Trans., on Industrial Informatics, vol:17, no.12, pp. 8080-8091, December 2021.